

See discussions, stats, and author profiles for this publication at: <https://www.researchgate.net/publication/257054120>

Proton beam writing. Mater Today

Article in *Materials Today* · June 2007

DOI: 10.1016/S1369-7021(07)70129-3

CITATIONS

193

READS

872

4 authors, including:



[Mark B. H. Breese](#)

National University of Singapore

272 PUBLICATIONS 5,282 CITATIONS

[SEE PROFILE](#)



[Jeroen A van Kan](#)

National University of Singapore

191 PUBLICATIONS 4,406 CITATIONS

[SEE PROFILE](#)



Proton beam writing

Proton beam (p-beam) writing is a new direct-writing process that uses a focused beam of MeV protons to pattern resist material at nanodimensions. The process, although similar in many ways to direct writing using electrons, nevertheless offers some interesting and unique advantages. Protons, being more massive, have deeper penetration in materials while maintaining a straight path, enabling p-beam writing to fabricate three-dimensional, high aspect ratio structures with vertical, smooth sidewalls and low line-edge roughness. Calculations have also indicated that p-beam writing exhibits minimal proximity effects, since the secondary electrons induced in proton/electron collisions have low energy. A further advantage stems from the ability of protons to displace atoms while traversing material, thereby increasing localized damage especially at the end of range. P-beam writing produces resistive patterns at depth in Si, allowing patterning of selective regions with different optical properties as well as the removal of undamaged regions via electrochemical etching.

Frank Watt*, Mark B. H. Breese, Andrew A. Bettioli, and Jeroen A. van Kan

Centre for Ion Beam Applications (CIBA), Physics Department, National University of Singapore, Singapore 117542

*E-mail: phywattf@nus.edu.sg

The rapid growth in nanotechnology coupled with the difficulties in fabricating structures below the 100 nm level has fueled an interest in the development of high-resolution lithographic technologies. Current microelectronics production technologies

are essentially two-dimensional, and are well suited for the two-dimensional topologies prevalent in microelectronics. As semiconductor devices are scaled down in size, and coupled with the integration of moving parts on a chip, there is expected to

be a rising demand for smaller microelectromechanical systems (MEMS) and nanoelectromechanical systems (NEMS) devices. High aspect ratio three-dimensional microstructures with nanometer details are also of growing interest for optoelectronic devices, and biochips using microfluidic channels are considered to have potential in the biomedical field.

Next-generation lithographies (NGLs) are actively being developed to take over from the highly successful optical lithography. As feature sizes shrink to well below 100 nm, diffraction limits imposed on the further development of optical lithography make it increasingly difficult to remain in step with Moore's law¹, although translating optical lithography to shorter wavelengths (e.g. extreme ultraviolet – EUV – lithography) alleviates such diffraction effects. Development of NGLs has focused on industrial production, and such masked lithographies (where primary radiation transmitting through large-area masks casts a pattern in a resist material) are considered the most efficient means of producing multiple and cheap components. More recently, however, direct-write technologies (where the primary radiation is focused to a small beam and scanned serially across a resist) have been considered as possible alternatives to masked technologies². Although the relatively low fabrication speed of direct-write technologies has been previously considered too slow for mass production, these serial techniques may have some distinct advantages when used to write stamps or molds and combined with nanoimprinting and pattern transfer^{3,4}.

The direct-write technologies currently employed for nanofabrication are, in general, based on charged particles that can be focused to nanodimensions, e.g. electrons (e-beam writing) and slow heavy ions (focused ion beam technology – FIB). Both these technologies have been highly successful, and e-beam writers and FIB instruments are available commercially. In e-beam writing, the primary interaction between the electron beam and the resist material is that of electron/electron collisions, which results in large-angle multiple scattering of the electron beam and the classic 'pear-shaped' ionization volume around the point of entry into the material. The electron trajectories can be simulated using Monte Carlo techniques such as Casino⁵. As an example, a focused 50 keV electron beam penetrates up to a depth of 40 µm in the resist poly(methyl methacrylate), or PMMA, with a 20 µm spread in the beam. Sub-100 nm e-beam writing therefore can only be realized in very thin resist layers, although high aspect ratio structures can be fabricated using additional steps, e.g. reactive ion etching. In FIB, the primary mechanism is that of momentum transfer between the slow-moving incident heavy ions and the atoms on the surface of the material. The surface atoms are rearranged, resulting in chemical and structural changes as well as sputtering of atomic and molecular species from the surface. The sputtering mechanism can be calculated using Monte Carlo techniques⁶, and the sputtering rate for a 30 keV Ga ion of around one to ten atoms for a wide variety of materials has been measured⁷. This

relatively slow rate of material removal compared with e-beam writing in resists imposes limitations on FIB as a rapid fabrication technique, and as such FIB is generally confined to specialist applications only.

Recent developments in high-energy (MeV) proton focusing in which sub-100 nm levels have been demonstrated⁸ have led to the emergence of a new direct-write nanofabrication technique – *p-beam writing*. P-beam writing is essentially an analogue of e-beam writing, but which utilizes the high mass properties of protons compared with electrons.

Physical properties of MeV protons

The trajectory of a MeV proton in a resist material is dependent on the interaction with both the atomic electrons and nuclei in the material. For most of its path, the probability that a proton interacts with an electron is a few orders of magnitude larger than for nuclear scattering and, as a first approximation, nuclear collisions have little effect on the trajectories⁶. Because of the high mismatch in mass between the proton and the material's electrons ($m_p/m_e \approx 1800$), proton collisions with electrons do not result in any significant deviation in the trajectory of a proton from a straight-line path. Further, because of the momentum mismatch, the energy transfer in each proton/electron collision is small and, consequently, many thousands of collisions will occur before a proton comes to rest. The primary interaction of high-energy protons (e.g. 500 keV – 3 MeV) is, therefore, that of deep penetration into the material with a minimal amount of surface disruption. In addition, diffraction effects are not an issue (the wavelength of a 100 keV proton is around 10^{-4} nm).

The interaction between a proton beam and matter can be summarized as follows:

- (i) The proton beam travels in a straight line apart from a small amount of end-of-range broadening (where nuclear collisions become more prominent). This offers a considerable advantage over e-beam writing for fabricating high aspect ratio three-dimensional structures, since a finely focused electron beam spreads rapidly as it enters the resist material.
- (ii) The exposure as the protons penetrate the material is relatively constant (apart from a ten-fold increase at the end of range). This feature offers an advantage over EUV or X-ray lithographies, which exhibit an exponential reduction in dose with depth.
- (iii) The penetration depth of the proton beam is well defined and can be varied by changing the proton beam energy. This is a unique characteristic that allows multilevel structures to be formed in one layer of resist.
- (iv) Lithography with protons also offers a virtual absence of high-energy secondary electrons that could otherwise give rise to unwanted exposure of the resist (proximity effects). In e-beam writing, for example, a small but significant fraction of secondary electrons are generated with energies that can contribute to the proximity effect in the micron range. Proton trajectories and

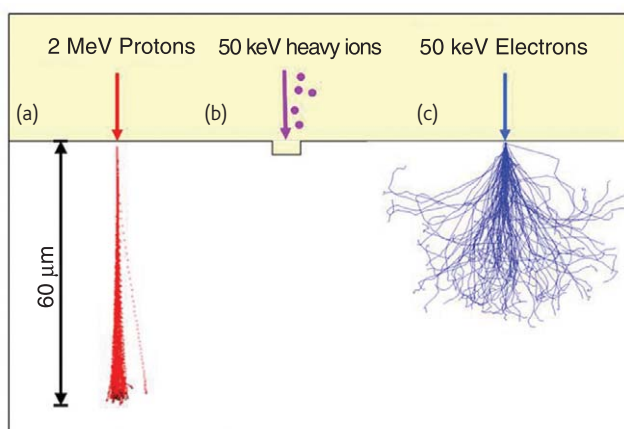


Fig. 1 Comparison between (a) p-beam writing, (b) FIB, and (c) e-beam writing. This figure shows schematically the difference between the three techniques. The p-beam and e-beam images were simulated using SRIM and CASINO software packages, respectively.

energy loss profiles can be accurately simulated by means of Monte Carlo calculations, for example using the computer code SRIM⁶, and e-beam writing can be simulated using the CASINO code⁵. A comparison between p-beam writing, FIB, and e-beam writing is shown in Fig. 1. Recent Monte Carlo calculations using the Hansen-Kobach-Stolterfoht model for proton-induced secondary electron emission⁹ indicate the superior nature of p-beam over e-beam writing with respect to the extent of proximity effects and penetration profiles. The simulations using the δ -simulator computer program show that the use of protons for lithography result in more confined energy density profiles along the proton beam trajectory (Fig. 2). From Fig. 2 it can also be observed that the energy distribution profiles from the proton beam trajectory over the first 2 μm of penetration into the resist is essentially contained within a 10 nm diameter, an improvement of several orders of magnitude compared with electrons.

The primary mechanisms for producing structures in resist materials is, in general, bond scissioning in positive resists such as PMMA, or cross-linking in negative resists such as SU-8. In positive resists the damaged regions are removed by chemical development to produce structures, whereas in negative resists the development procedures remove the undamaged resist leaving the cross-linked structures behind. In e-beam writing, the primary and secondary electrons create the scissioning or cross-linking, whereas in p-beam writing the damage is caused by proton-induced secondary electrons. The proton dose required for exposure varies from 30–150 nC/mm² depending on the resist material¹⁰, and is around 80–100 times less than that required by e-beam writing^{11–13}. Protons have an added feature that is not applicable to e-beam writing. Energetic protons can induce atomic displacements in crystalline materials, which in turn can alter the local electrical properties. For example, as a 2 MeV proton penetrates Si, it loses energy and eventually comes to rest $\sim 48 \mu\text{m}$ below the surface.

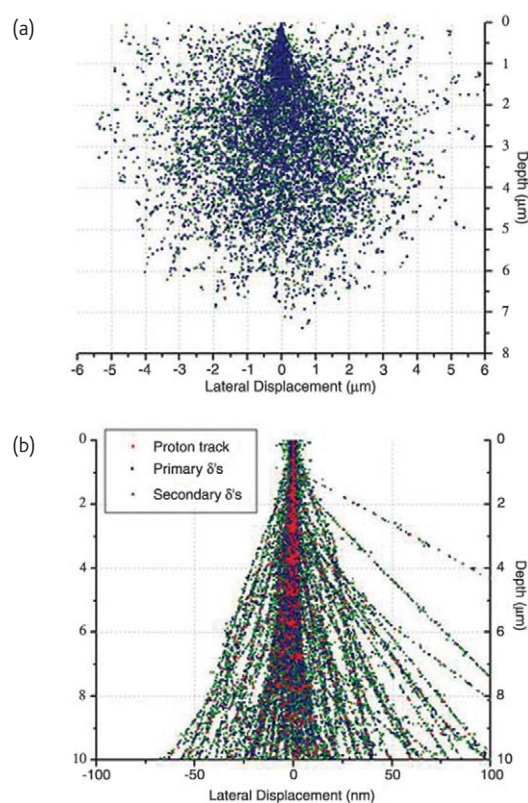


Fig. 2 (a) δ -simulator profiles of one thousand 20 keV electrons penetrating a 10 μm thick PMMA layer (primary electrons are shown in red, secondary electrons in green). (b) δ -simulator profiles of one thousand 2 MeV protons penetrating a 10 μm thick PMMA layer (primary protons are shown in red, secondary electrons in green). Note the vastly different lateral displacement scales along the x-axis in the two cases. (Reproduced with permission from⁹. © 2007 Elsevier.)

Si vacancies are created along the proton path, with most of the damage produced at the end of range. According to SRIM calculations (Fig. 3), a dose of 5×10^{15} protons/cm² at an energy of 2 MeV will introduce a defect concentration of $\sim 10^{19}$ vacancies/cm³ close to the surface, increasing sharply to a maximum of 10^{20} vacancies/cm³ at the end of range. This feature can be used to produce three-dimensional structures in bulk p-type Si, as well as altering the light-emitting optical properties to produce light-emitting patterns in porous Si. In addition, by using the increase in the end-of-range damage, p-beam writing can also be used to create changes in refractive index deep in materials such as polymers and Er³⁺-Yb³⁺ codoped phosphate glasses to produce buried waveguide amplifiers. Such applications are described later.

Current performance of p-beam writing

P-beam writing has been pioneered by the Centre for Ion Beam Applications (CIBA) at the National University of Singapore. The technology, which uses a MeV proton beam focused to small spot sizes and scanned across a resist, is similar to that developed for nuclear microscopy and nuclear microprobe applications using MeV protons¹⁴. A small particle accelerator provides a stable beam of MeV ions that is

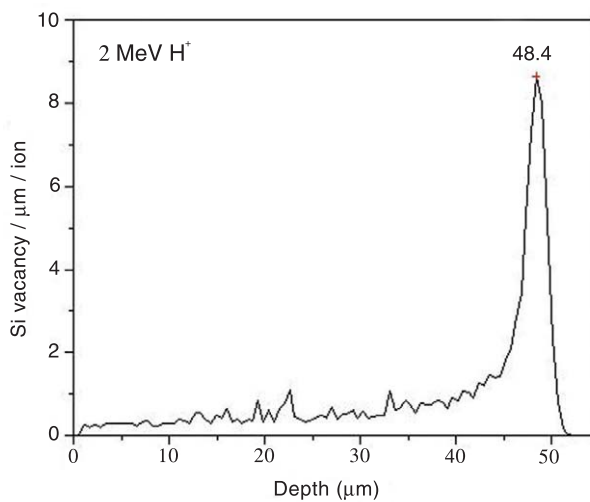


Fig. 3 SRIM calculation of the vacancy profile for 2 MeV protons in Si. (Reproduced with permission from⁵⁶. © 2004 SPIE.)

focused using a system of strong focusing quadrupole lenses. In nuclear microscopy, the beam is scanned across a specimen to yield information such as trace elemental images (e.g. in biological tissue) and images of crystalline quality (e.g. three-dimensional defect mapping of advanced materials). In p-beam writing, the beam is scanned across a resist material in a predetermined pattern, which is subsequently developed to produce three-dimensional structures. Technical and commercial development has been hampered in the past by the difficulties encountered in focusing MeV ions to sub-100-nm dimensions. However, with the advent of compact magnetic quadrupole lens systems, these difficulties have recently been overcome⁸ and the first prototype p-beam writer has recently been designed and constructed at CIBA¹⁵. The CIBA setup, which is capable of producing a sub-100-nm MeV proton beam, is shown schematically in Fig. 4.

Most of the early p-beam written structures^{16–21} were fabricated in PMMA, a polymer resist widely used in e-beam writing (Fig. 5a). Subsequently, a variety of resist materials have been tested^{22–24} and

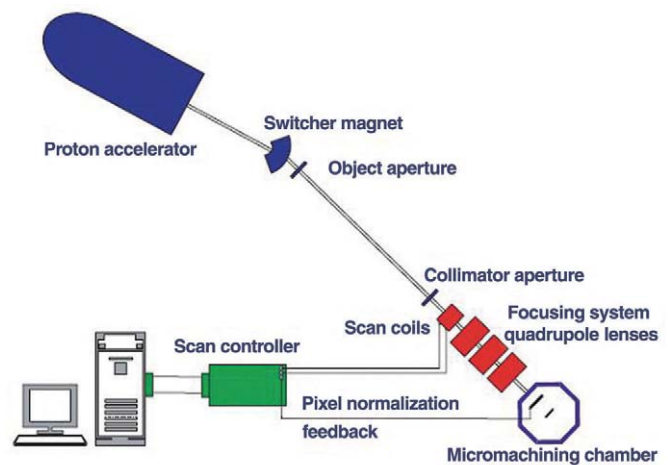


Fig. 4 Schematic of the p-beam writing facility at CIBA. MeV protons are produced in a proton accelerator, and a demagnified image of the beam transmitted through an object aperture is focused onto the substrate material (resist) by means of a series of strong focusing magnetic quadrupole lenses (e.g. quadrupole triplet). Beam scanning takes place using magnetic or electrostatic deflection before the focusing lenses, and is driven by a feedback signal derived from the proton interactions with the resist. This feedback mechanism ensures a constant beam exposure per pixel as the beam is scanned across the resist, resulting in high-quality structures.

high aspect ratio test structures at the nanolevel have been written in both SU-8 and hydrogen silsesquioxane (HSQ) (Figs. 5b and 5c)^{25–27}. The penetration depth of the proton beam depends on its energy, and this feature has been used to produce multilevel structures (Figs. 6a and 6b). These test structures are fabricated by using different proton energies in one layer of resist, which is subsequently developed. Several groups have also produced subsurface channels and tunnel structures^{28–30}, demonstrating the flexibility of p-beam writing. When polytetrafluoroethylene (PTFE) is exposed to MeV protons in an oxygen-rich atmosphere (e.g. air), it is possible to create holes of millimeter depths, much greater than the penetration depth of the incident protons. The hole diameters are defined by the beam scan

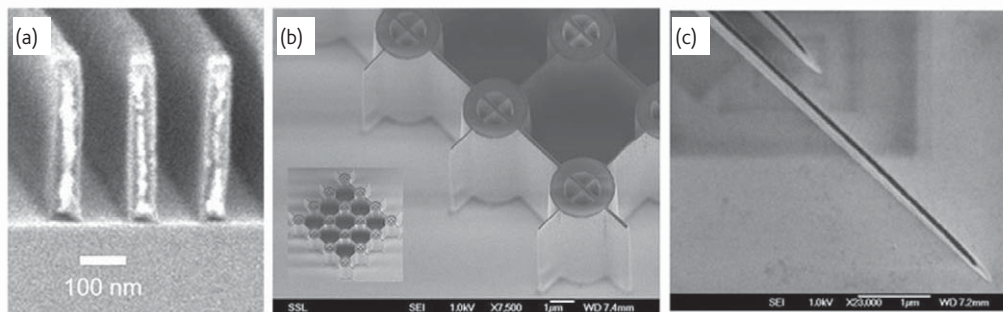


Fig. 5 (a) Scanning electron microscopy (SEM) image of parallel lines written in a 350 nm thick PMMA layer. The structure was written with a focused 2 MeV proton beam, and the structure has a wall width of 50 nm. (b) High aspect ratio test structures fabricated using p-beam writing in SU-8 negative resist showing 60 nm wall structures that are 10 μm deep. (Parts (a) and (b) reproduced with permission from²⁷. © 2004 Inderscience Publishers.) (c) P-beam written test structures in hydrogen silsesquioxane, which has been tested as a superior resist for p-beam writing, allowing the production of high aspect ratio structures down to 22 nm. (Reproduced with permission from²⁵. © 2006 American Chemical Society.)

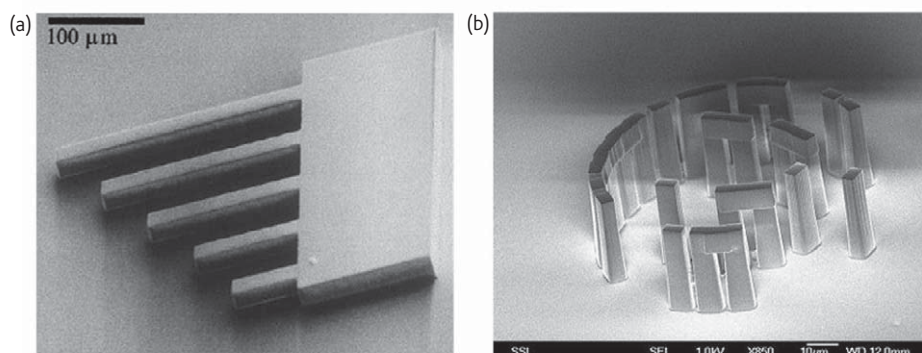


Fig. 6 (a) SEM image of a set of cantilevers produced in a 36 μm thick SU8 layer. The suspended cantilevers were produced using a 1.0 MeV proton exposure and the anchor was exposed using 2.0 MeV protons. (Reproduced with permission from²⁷. © 2004 Inderscience Publishers.) (b) Microsized copy of Stonehenge in the UK fabricated using p-beam writing in SU8 resist. By using the different depth exposure of two different proton energies, 500 keV for fabricating the horizontal slabs and 2 MeV for exposing the vertical supports, the complete structure can be fabricated in one layer of resist.

area on the PTFE surface³¹. The authors propose that the erosion is a result of the formation of a stable gaseous compound following beam-induced decomposition of the PTFE (possibly an acyl fluoride) that does not redeposit in the hole.

Application areas

The current application areas of p-beam writing are those that use the prime features of p-beam writing, i.e. precise three-dimensional fabrication in resist materials and the ability of protons to produce atomic displacement and damage at specific depths in the sample.

Photonics

Waveguides

Optical waveguides represent an integral part of many microphotonic devices ranging from optical amplifiers, optical switches, and ring resonators, to interferometers³². Two types of waveguiding structures have been fabricated using p-beam writing. The first type involves direct fabrication of a high refractive index core followed by coating with a lower refractive index cladding layer. This procedure has been used to make both single and multimode waveguides in polymers³³, examples of which are shown in Figs. 7a and 7b. Waveguides fabricated in this way exhibit low transmission loss (estimated at 0.19 dB/cm at 632.8 nm) because of the smooth sidewalls and low edge roughness of the p-beam written structures³⁴. The sidewall smoothness of these waveguides has been measured to be ~ 4 nm³⁵.

The second fabrication technique relies on the property that MeV protons traveling into a sample will lose most of their energy and cause most damage in the sample at the end of range. This beam-induced damage causes a volume change at the end of range, resulting in increased density and increased refractive index³⁶. In order to achieve weak guiding of light, a refractive index contrast of about 10^{-4} – 10^{-3} is usually sufficient, depending on the material being used. The p-beam writing technique has also recently been applied to the fabrication of buried channel waveguides in phosphate glass that has been co-doped

with Er^{3+} and Yb^{3+} to produce optical amplifiers with a maximum net gain of 1.72 dB/cm measured at a wavelength of 1.534 μm ³⁷.

Lens arrays

P-beam writing has the flexibility to fabricate microlens arrays using the thermal reflow process³⁸ without the need for a high aspect ratio mask. Firstly, a layer of photoresist is spin coated onto a transparent substrate (e.g. a glass slide or coverslip) and patterned using p-beam writing. The exposed regions are then removed to leave behind an array of cylinders with diameters corresponding to that of the required final lens. The cylindrical structures are then heated to a temperature well above the glass transition temperature of the polymer but below the disintegration temperature. During the heating process, the polymer flows and the surface tension forms a hemispherical surface on the substrate. This process has been used to fabricate microlens arrays in PMMA³³. The p-beam writing technique has also been used in conjunction with Ni electroplating to fabricate microlens array molds and stamps. These stamps have been used to replicate microlens arrays in polymers such as polydimethylsiloxane (PDMS) and polycarbonate³⁹.

Gratings

The ability of p-beam writing to produce vertical and smooth sidewalls in resist materials, coupled with a low line-edge roughness, makes it an ideal technique for many microphotonic devices. Gratings have been fabricated in various thickness of PMMA³³. Fig. 7c shows a grating fabricated in an 800 nm layer of PMMA spin coated onto a Si wafer that has been previously coated with a Cr (20 nm)/Au (200 nm) seed layer. The metallic seed layer in these samples assists the adhesion of the PMMA to the Si substrate, although for the production of metallic gratings this layer can also act as a seed layer for electroplating. The extremely low line-edge roughness can be easily observed in these images, indicating that higher density lines and spaces are possible with the p-beam writing technique.

Colloidal crystal templates

In 1987, Yablonovitch⁴⁰ and John⁴¹ showed that electromagnetic radiation interacting with a periodic dielectric structure with a lattice

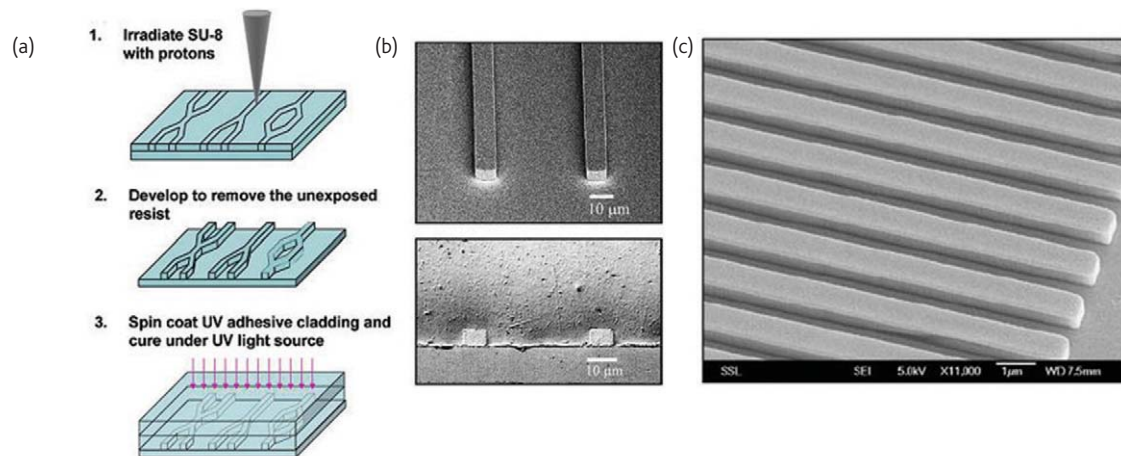


Fig. 7 (a) Fabrication procedure for ridge-type waveguides fabricated in SU-8. (b) SEM images of an SU-8 Y-branch made using p-beam writing, before and after the cladding layer is added. (c) SEM images of a surface relief grating fabricated in an 800 nm layer of PMMA spin coated onto a Si wafer with a Cr (20 nm)/Au (200 nm) seed layer. (Reproduced with permission from³³. © 2005 Elsevier.)

constant of the order of the wavelength of the radiation exhibits behavior analogous to electrons in a crystalline material. This discovery has led to a surge of interest in the development of new micro-optical systems, since the ability to control light in three dimensions will lead to numerous applications in the field of optoelectronics and microphotonics. These photonic crystals can be used to make waveguides with 90° bends, enhance the emission from light-emitting diodes⁴², and fabricate optical fibers that have air as a core material⁴³. One way of fabricating photonic crystals uses the crystallization of a monodisperse colloidal system to create a three-dimensional lattice of micro- and nanospheres. Because p-beam writing can write precise and accurate three-dimensional structures with vertical walls and low edge roughness, it has been shown to be a useful tool for the fabrication of polymeric templates for directed self-assembly³³. The precision of the high aspect ratio template structures that can be machined using p-beam writing can be used to support more layers than are otherwise possible with standard colloidal crystallization techniques.

Microfluidic devices, biostructures, and biochips

The ability of p-beam writing to create smooth three-dimensional channels in polymers allows the direct writing of microfluidic devices. Microchannels down to 100 nm wide in PMMA have been fabricated and a surface smoothness of 2.5 nm for the sidewalls of the channels has been measured using atomic force microscopy (AFM). Characterization of the channels' electrokinetic behavior has been undertaken⁴⁴, and a theoretical model developed to predict the bulk electro-osmotic flow of phosphate buffer solution in the channels has shown good agreement with the measured electro-osmotic mobilities. Encapsulation of the microchannels to avoid fluid evaporation is an important factor in fabricating a working system, and thermal bonding techniques to produce enclosed proton-written nanochannels have proved successful⁴⁵.

In work involving the behavior of cells (fibroblasts) in a three-dimensional micro-environment, p-beam writing has been used to fabricate a cell 'corral' consisting of a circular wall with four 'outlet channels' of differing widths enclosing a flat surface⁴⁶. Cells seeded onto the circular flat surface migrate outward to the inside wall of the corral, where further migration is retarded. Cells pass through the outlet channels one by one, at a migration speed dependent on the width of the channels.

The ability of p-beam writing to write deep channels with widths below 100 nm demonstrates the potential of fabricating biochips that can sort cells, DNA, and large proteins. An example of a test chip created using p-beam writing is shown in Fig. 8, which operates through the process of entropic trapping⁴⁷. In the p-beam written chip,

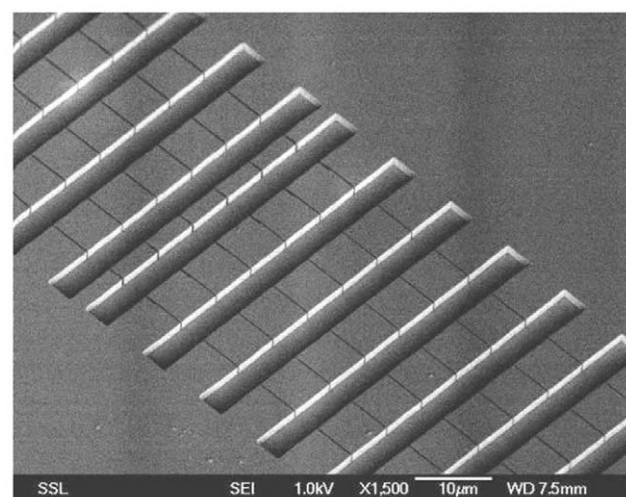


Fig. 8 A series of reservoirs connected by 100 nm wide channels. When an electric field is applied along the channels, DNA is stretched through the nanochannels at a rate that depends on the size and unfolding characteristics of the DNA.

DNA is trapped in a series of reservoirs that are interconnected by 100 nm channels. When an electric field is applied along the channels, the DNA molecules uncoil and pass through the channels at a rate that depends on size and unfolding parameters.

Imprinting

Direct-write fabrication of devices and structures, by its nature, is carried out in a serial manner and, as such, is not conducive to the mass production of devices. However, the use of imprinting techniques, which can replicate structures quickly and cheaply, is beginning to show promise. The use of direct writing to fabricate stamps and molds that can be used as imprinting masters therefore offers the possibility of fabricating structures that may be commercially competitive with those produced by masked processes. P-beam writing, which is able to produce structures with vertical and smooth sidewalls in resist

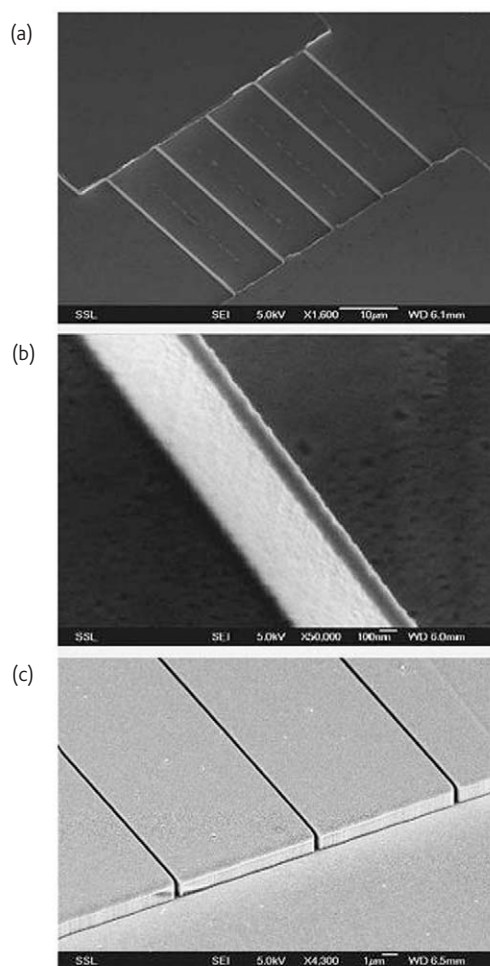


Fig. 9 (a) A low-magnification SEM image of a Ni nanostamp fabricated using p-beam writing and Ni electroplating. The stamp is a test pattern featuring two raised platforms connected by five 100 nm wide, 2 μm deep, 30 μm long high aspect ratio ridges. (b) A high magnification image of a 100 nm Ni ridge, exhibiting vertical sidewalls. (c) An imprint of the above Ni stamp in 8 μm thick PMMA spin coated on a Si substrate showing reproducible fine features, smooth sidewalls, and vertical structures. (Reproduced with permission from⁴⁸. © 2005 Elsevier.)

material, is an ideal technique for fabricating three-dimensional structures suitable for molds and stamps. The p-beam written structures can be subsequently transformed into metal negatives using electroplating techniques. Figs. 9a and 9b indicate the precision at which these metallic stamps can be fabricated, in this case using a single step nickel sulfamate plating process on p-beam written PMMA three-dimensional patterned structures. Nanoindentation and AFM measurements of surface features on the stamp indicate a hardness of 5 GPa and a sidewall roughness of 7 nm. Fig. 9c indicates the high quality and reproducibility of the pattern after being transferred into PMMA^{48,49}. The imprint lithography was carried out with a commercial nanoimprinter (Obducat Technologies NIL-2-PL 2.5 nanoimprinter) using hot-embossing lithography.

P-beam modification of Si

P-beam writing in Si results in a patterned damage profile that can be used in a variety of ways. It has been used for producing micropatterned Si surfaces, controlled photoluminescence from patterned porous Si, and controlled reflectivity from patterned porous Si Bragg reflectors. Fig. 10 indicates the process used.

First, a finely focused beam of MeV ions⁵⁰ is scanned over the Si wafer surface (Fig. 10a). The ion beam loses energy as it penetrates the semiconductor and comes to rest at a well-defined range. The stopping

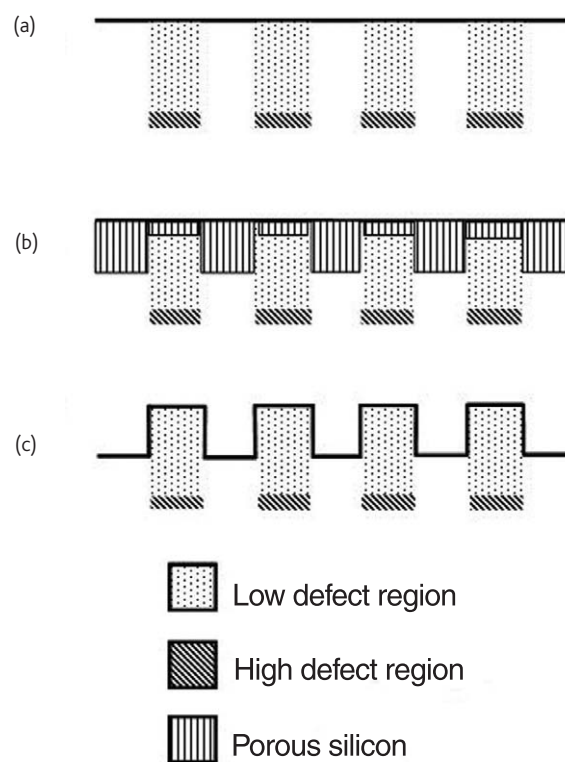


Fig. 10 (a) Patterning of p-type Si with p-beam writing; (b) electrochemical etching to selectively form patterned porous Si; and (c) removal of porous Si with dilute KOH solution to form a micromachined structure.

process damages the Si crystal by producing additional vacancies in the semiconductor⁵¹. A higher beam dose produces a higher vacancy concentration, so by pausing the focused beam for different amounts of time at different locations, any pattern of localized damage can be built up. The irradiated wafer is then electrochemically etched in a dilute solution of HF (Fig. 10b). An electric current is passed through the wafer, which forms porous Si at the surface. The buried regions of high vacancy concentration inhibit this formation process, so a thinner layer of porous Si is produced at the irradiated regions. A very large beam dose may reduce the etch rate to zero in the irradiated regions. The etched sample comprises patterned areas of porous Si that may emit light with greater or lesser intensity, or different wavelength, compared with the surrounding unirradiated regions. If the anodization is repeated with alternating low and high current densities then the range of wavelengths of incident light reflected from the resultant Bragg reflector depends on the irradiation dose. If the etched sample is immersed in KOH the porous Si is removed, leaving the patterned structure on the wafer surface as a three-dimensional representation of the scanned pattern and dose (Fig. 10c).

Si microfabrication

Many new technologies require the fabrication of precise three-dimensional structures in Si^{52,53}. Electrochemical etching of Si in HF is emerging as an alternative technique for micromachining because of its low cost, fast etching speed, and easy implementation. Recent results on fabricating high aspect ratio, multilevel structures in Si have been published^{54–56}. Figs. 11a and 11b shows scanning electron microscopy (SEM) images of a linear waveguide with a grating at the top surface with a 1 μm period. This is designed to transmit a certain infrared (IR) wavelength along the waveguide while the grating selects which wavelengths are transmitted, depending on the periodicity. This waveguide was formed by first fabricating the waveguide using the micromachining process described above, then spinning on a layer of polymer resist and creating a grating in the polymer using a second irradiation stage with a beam spot focused to 100 nm or less. The pattern is then transferred to the Si waveguide top surface using reactive ion etching.

After etching beyond the end of range of the ions, the isotropic electrochemical etching process starts to undercut the irradiated structure, so multilevel micromachined structures can be created by irradiating with two different proton energies. Regions irradiated with lower energies become undercut at a shallower etch depth, while regions irradiated with higher energy protons continue to increase in height, so multilevel freestanding microstructures can be fabricated in a single etch step. To demonstrate this, bridge structures have been irradiated with 0.5 MeV protons (range $\sim 6 \mu\text{m}$) and supporting pillars with 2 MeV protons (range $\sim 48 \mu\text{m}$). Fig. 11c shows the resultant Stonehenge-like structure after prolonged etching, in which the bridges are fully undercut and separated from the substrate but are supported by the irradiated pillars.

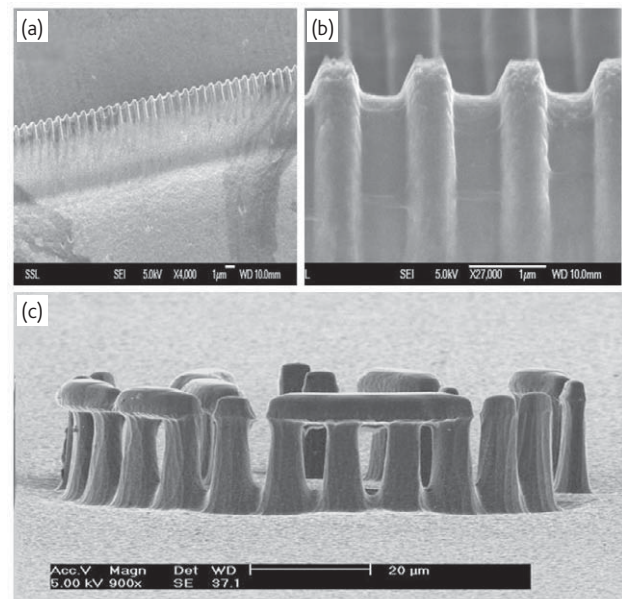


Fig. 11 SEM images of (a) a linear waveguide with a grating at the top surface with a 1 μm period; and (b) at higher magnification. (c) Micromachined Stonehenge-like structure, 80 μm in diameter.

Porous Si patterning

Porous Si is of interest because of its photoluminescence (PL) and electroluminescence (EL) properties^{57,58}, raising the possibility of producing light-emitting devices with microelectronics compatibility. A potentially important application of porous Si is the production of combined optical/electronic devices incorporating patterned porous material directly onto a Si substrate with high spatial resolution. We have undertaken a comprehensive study of the effects of ion irradiation on a wide range of different resistivity *p*-type Si wafers, and recorded the resultant PL intensity and wavelength^{59–61}. There are two resistivity regimes of *p*-type Si where PL is affected in different ways by ion irradiation: for low resistivity ($\sim 0.01 \Omega\cdot\text{cm}$) wafers irradiation primarily results in a large PL increase, whereas for moderate resistivity ($0.1\text{--}10 \Omega\cdot\text{cm}$) wafers irradiation primarily results in a large PL wavelength red shift. A demonstration of this different behavior is shown in Figs. 12a and 12b. In low resistivity *p*-type Si, the irradiated dragon produces bright, red PL compared with the faint unirradiated background. In moderate resistivity Si, bright orange/red PL is produced from the dragon, whereas the background produces green PL of a similar intensity. In Fig. 12c, a range of doses have been irradiated in a continuous distribution in moderate resistivity Si, producing a gradual change in PL emission wavelength. Fig. 12d shows a PL image of the painting *The Ancient of Days* by William Blake, reproduced in porous Si. The dose of each region was adjusted so that the PL color emission from the porous Si resembles the original as closely as possible.

Distributed Bragg reflectors in porous Si

The refractive index of porous Si is lower than for bulk Si: it is inversely proportional to the anodization etch current density. A distributed

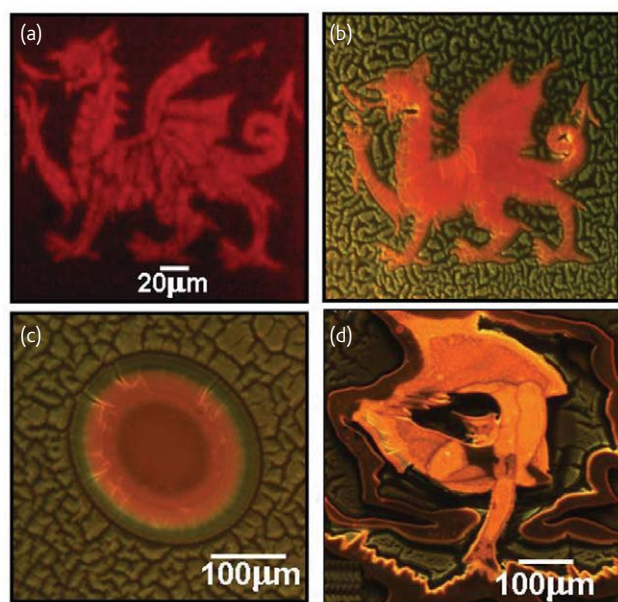


Fig. 12 PL images of dragons formed by irradiating a p-type Si (a) 0.02 Ω .cm wafer and (b) 3 Ω .cm wafer. (c) Concentric ring patterns in a 3 Ω .cm Si wafer formed by linearly increasing the dose from the outer edge to the center. (d) The Ancient of Days by William Blake, fabricated in a $500 \times 500 \mu\text{m}^2$ area of 3 Ω .cm Si. The picture was irradiated with a dose of 5×10^{13} for black, 1×10^{13} for red, 5×10^{12} for orange and 1×10^{12} for yellow-green. (Reprinted with permission from⁶¹. © 2006 Wiley-VCH.)

Bragg reflector (DBR) selectively reflects a band of incident wavelengths and is easily formed in highly doped p-type Si by periodically lowering and raising the etch current density, resulting in a sequence of porous layers with alternating high and low refractive index.

Fig. 13a shows an optical image of a $500 \times 500 \mu\text{m}^2$ region irradiated with different overlaid scan patterns, with different doses⁶². The wafer was etched with an alternating high/low current density for 4 s per layer, with a total of 15 bilayers formed. The etch rate is progressively slowed by larger irradiation doses, resulting in thinner porous layers that reflect shorter incident wavelengths. Each dose produces a different reflected color when illuminated with white light, with red/orange colors corresponding to areas of lowest dose. The potential of this approach to form patterned arrays of color pixels and lines for display applications is shown in Fig. 13b, where vertical lines, each 10 μm wide, were irradiated to form alternating red-green-blue stripes. Figs. 13c and 13d shows examples of selectively patterning color reflective areas in which two dragon images appear in different colors, corresponding to different irradiated doses in each area.

Magnetic writing in carbon

Ferromagnetic microstructures, caused by localized ferromagnetic ordering, have been written in highly oriented pyrolytic graphite (HOPG) using a beam of 2.25 MeV protons, and characterized using AFM/magnetic force microscopy (MFM) and superconducting quantum interferometer device (SQUID) measurements^{63,64}. Although the

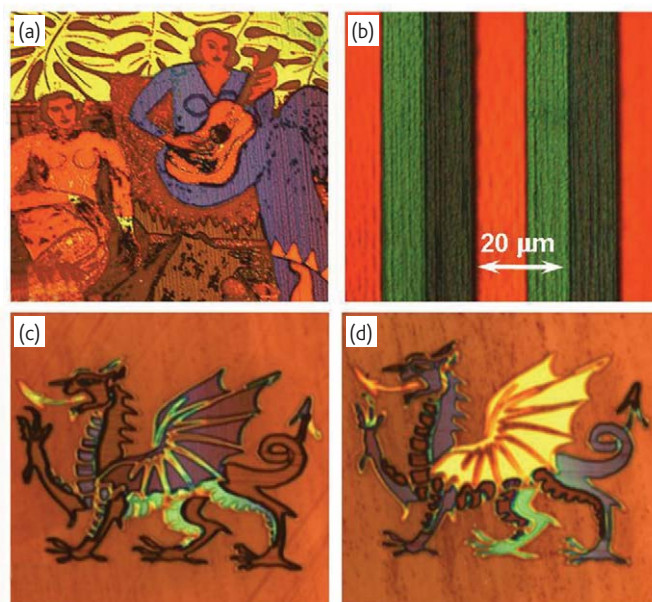


Fig. 13 Optical reflection images of (a) the painting La Musique by Henri Matisse (1939) created by irradiating a $500 \times 500 \mu\text{m}^2$ area. (b) Vertical lines, each 10 μm wide, irradiated to form alternating red-green-blue stripes. (c), (d) $500 \times 500 \mu\text{m}^2$ areas showing two dragon images corresponding to different irradiated doses in each area. In each recorded image the sample was illuminated with white light and the reflected light was recorded for 30 s. (Reprinted with permission from⁶². © 2006 American Institute of Physics.)

mechanism of the ordering in carbon by protons is not known in detail, experimental evidence and theoretical predictions suggest that the effect is caused by lattice disorder created by protons coupled with the implantation of the residual protons (as hydrogen). Further work has indicated that superparamagnetic spots in polyimide foils can also be created by proton microbeam irradiation, leading the authors to conclude that the fabrication of magnetic structures of more complex shapes, and the creation of ferromagnetic nanotips by irradiating single carbon nanotubes, could lead to very useful applications of p-beam writing in the future⁶⁵.


Conclusions

P-beam writing is underdeveloped technically compared with e-beam writing and FIB technology. In spite of this, p-beam writing is now capable of writing high aspect ratio structures down to the 20 nm level in resist material, achieved using the prototype p-beam writer at the CIBA at the National University of Singapore. The structures produced have smooth and vertical sidewalls, with a depth of fabrication dependent on the proton beam energy. Because of its minimal proximity effects, p-beam writing has the capability of producing structures of high packing density.

P-beam writing is a direct-write process and, as such, is not considered suitable for mass production of devices. The transfer of large-scale patterns using nanoimprinting, however, represents a technique of great potential for the mass production of a new

generation of large area, high-density, low-dimensional structures. The potential role of imprint lithography for mass production depends crucially on the quality of stamps that can be fabricated, and p-beam writing appears ideal for producing high aspect ratio metallic stamps of precise geometry.

Focused MeV proton beams may also be used to produce high aspect ratio, multilevel microstructures in Si by using the ability of protons to modify the local properties of Si through vacancy production. The feature heights of the irradiated structure can be accurately controlled with the incident beam dose, enabling the production of a multilevel structure by multiple dose exposures in a single irradiation. P-beam writing can also be used to produce patterned porous Si for a range of different applications. Tuning of the PL intensity and wavelength has been obtained by controlling the local resistivity as a function of dose.

P-beam writing is a new technology of great potential, and both current experimental data and theoretical predictions indicate that sub-10-nm structuring is feasible. The primary physical characteristics of MeV proton beams, that of high penetration with little lateral beam spreading, make p-beam writing the only true direct-write, three-dimensional fabrication technique at the nanoscale. The high mass of the proton compared with the electron produces minimal proximity effects, and hence p-beam writing has more potential for fabricating structures at the nanometer level than e-beam writing. The further development of p-beam writing, which is still in its infancy, will be an exciting venture requiring the development of high-brightness proton sources and more stable ion accelerators in order to achieve nanometer resolution. The lack of a user-friendly commercial instrument is currently holding back the potentially wide range of application fields in which p-beam writing could make a substantial impact. Hopefully, this will be addressed in the near future. 

REFERENCES

- Moore, G. E., *Electronics* (1965) **38**, 114
- International Technology Semiconductor Roadmap* (2003), <http://public.itrs.net/Files/2003ITRS/Home2003.htm>.
- Xia, Y., and Whitesides, G. M., *Angew. Chem. Int. Ed.* (1999) **37**, 550
- Pease, R. F., *Nature* (2002) **417**, 802
- Hovington, P., *Scanning* (1997) **19**, 29
- Ziegler, J. F., *The Stopping and Range of Ions in Matter*, Vols. 2-6, Pergamon, Oxford, (1977-1985)
- Reyntjens, S., and Puers, R., *J. Micromech. Microeng.* (2001) **11**, 287
- Watt, F., et al., *Nucl. Instr. Meth. Phys. Res. B* (2003) **210**, 14
- Udalagama, C. N. B., et al., *Nucl. Instr. Meth. Phys. Res. B* (2007), in press
- van Kan, J. A., et al., *Nucl. Instr. Meth. Phys. Res. B* (2007), in press
- Saifullah, K. R. V., et al., *Nano Lett.* (2003) **3**, 1587
- Namatsu, H., et al., *Microelectron. Eng.* (1998) **41-42**, 331
- Adesida, I., *Nucl. Instr. Meth. Phys. Res. B* (1985) **7-8**, 923
- Watt, F., and Grime, G. W., *Applications of Nuclear Microprobes*, Adam Hilger, Bristol, (1987)
- van Kan, J. A., et al., *Appl. Phys. Lett.* (2003) **83**, 1629
- Breese, M. B. H., et al., *Nucl. Instr. Meth. Phys. Res. B* (1993) **77**, 169
- Springham, S. V., et al., *Nucl. Instr. Meth. Phys. Res. B* (1997) **130**, 155
- Sanchez, J. L., et al., *Nucl. Instr. Meth. Phys. Res. B* (1998) **136-8**, 385
- van Kan, J. A., et al., *Nucl. Instr. Meth. Phys. Res. B* (1999) **148**, 1085
- Watt, F., *Nucl. Instr. Meth. Phys. Res. B* (1999) **158**, 165
- van Kan, J. A., et al., *Nucl. Instr. Meth. Phys. Res. B* (1999) **158**, 179
- de Kerckhove, D. G., et al., *Nucl. Instr. Meth. Phys. Res. B* (1998) **136-8**, 379
- Gomez Morriilla, I., et al., *J. Micromech. Microeng.* (2005) **15**, 706
- Rajta, I., et al., *Nucl. Instr. Meth. Phys. Res. B* (2005) **231**, 423
- van Kan, J. A., et al., *Nano Lett.* (2006) **6**, 579
- van Kan, J. A., et al., *Improvement in Proton Beam Writing at the nano scale*, *Proc. 17th IEEE Int. Conf. Micro Electro Mechanical Systems* (2004), 673
- van Kan, J. A., et al., *Int. J. Nanotechnol.* (2004) **1**, 464
- Simčič, J., et al., *Nucl. Instr. Meth. Phys. Res. B* (2005) **241**, 479
- Glass, G. A., et al., *High energy Focused Ion beam Nanoprobes: Design and Application*. In *Growth, Modification, and Analysis by Ion Beams at the Nanoscale*, Joerg, K. N., et al., (eds.), *Mater. Res. Soc. Symp. Proc. 908E* (2006), 0006-01
- Gonin, Y., et al., *Appl. Surf. Sci.* (2003) **217**, 289
- Gomez Morriilla, I., et al., *J. Micromech. Microeng.* (2005) **15**, 698
- Prieto, F., et al., *Nanotechnology* (2003) **14**, 907
- Bettiol, A. A., et al., *Nucl. Instr. Meth. Phys. Res. B* (2005) **231**, 364
- Sum, T. C., et al., *Appl. Phys. Lett.* (2003) **83**, 1707
- Sum, T. C., et al., *Appl. Phys. Lett.* (2004) **85**, 1398
- Roberts, A., and von Bibra, M. L., *J. Lightwave. Technol.* (1996) **14**, 2554
- Liu, K., et al., *Appl. Phys. Lett.* (2004) **84**, 684
- Borrelli, N., *Microoptics Technology: Fabrication and Applications of Lens Arrays and Devices*. Marcel Dekker Inc., New York, (1999)
- Dutta, R. K., et al., *Nucl. Instr. Meth. Phys. Res. B* (2007), in press
- Yablonovitch, E., *Phys. Rev. Lett.* (1987) **58**, 2059
- John, S., *Phys. Rev. Lett.* (1987) **58**, 2486
- Wierer, J. J., et al., *Appl. Phys. Lett.* (2004) **84**, 3885
- Russell, P., *Science* (2003) **299**, 358
- Ansari, K., et al., *J. Micromech. Microeng.* (2006) **16**, 1170
- Shao, P. E., et al., *Appl. Phys. Lett.* (2006) **88**, 093515
- Sun, F., et al., *Tissue Eng.* (2004) **10**, 267
- Han, J., et al., *Phys. Rev. Lett.* (1999) **83**, 1688
- Ansari, K., et al., *Nucl. Instr. Meth. Phys. Res. B* (2005) **231**, 407
- Ansari, K., et al., *J. Micromech. Microeng.* (2006) **16**, 1967
- Breese, M. B. H., et al., *Materials Analysis using a Nuclear Microprobe*, Wiley, New York, (1996)
- Breese, M. B. H., *Phys. Rev. B* (2006) **73**, 035428
- Nagata, S., et al., *Appl. Phys. Lett.* (1998) **72**, 2945
- Craighead, H. G., *Science* (2000) **290**, 1532
- Teo, E. J., et al., *Appl. Phys. Lett.* (2004) **84**, 3202
- Teo, E. J., et al., *Nucl. Instr. Meth. Phys. Res. B* (2004) **222**, 513
- Teo, E. J., et al., *Proc. SPIE* (2004) **5347**, 264
- Cullis, A. G., et al., *J. Appl. Phys.* (1997) **82**, 909
- Ossicini, S., et al., *Light-Emitting Silicon for Microphotonics*, Springer-Verlag, Berlin, (2003)
- Teo, E. J., et al., *Appl. Phys. Lett.* (2004) **85**, 4370
- Mangaiyarkarasi, D., et al., *J. Electrochem. Soc.* (2005) **152**, D173
- Teo, E. J., et al., *Adv. Mater.* (2006) **18**, 51
- Mangaiyarkarasi, D., et al., *Appl. Phys. Lett.* (2006) **89**, 021910
- Esquinazi, P., et al., *Phys. Rev. Lett.* (2003) **91**, 227201
- Spemann, D., et al., *Nucl. Instr. Meth. Phys. Res. B* (2005) **231**, 433
- Spemann, D., et al., *Nucl. Instr. Meth. Phys. Res. B* (2006) **250**, 303